第17卷 第4期
1995年12月

地 震 地 质
SEISMOLOGY AND GEOLOGY

Vol. 17 No. 4
Dec. 1995

地震前异常的阶段性及其空间分布特征*

马 瑾 马胜利 刘力强
(国家地震局地质研究所, 北京 100029)

摘 要 将岩石变形曲线到达强度点以前比拟为地震前异常的中长期阶段,强度点至失稳点之间定义为短临阶段。在中长期阶段异常是由驱动力的增强或区域应力场的调整引起,前者引起的应力扰动场与原来的方向一致,强烈扰动区与原来的应力集中区一致,后者引起的应力扰动场应力方向可以发生变化,应力扰动对平均应力影响较大,强烈扰动区位于断层错列部位。二者的强烈扰动场均与未来的震源区无必然联系。在短临阶段异常是由局部断层扩展或弱化引起,与之相伴的是平均应力扰动场的四象限分布和最大剪应力扰动场的八瓣式分布。

主题词: 地震前兆 异常识别 长期异常 中期异常 短临异常 空间分布特征

1 前 言

在地震前的一段时间内和一定区域范围内往往出现一些异常,临近地震时在震区附近也出现一些异常。有人称前者为"中长期前兆",后者则被称为"短临前兆"[1]。与此同时,一些学者把震前较大范围(也在较长时期中)出现的异常称为"场兆",而把发震地点附近的异常称为"源兆"。然而,多年来的地震事实表明:不是所有地震前都能发现"前兆";不同地区,甚至同一地区不同时段出现的"前兆"也不相同[2];同一地震前的"中长期前兆"和"短临前兆"往往不出现在同一地区[3]。因此,很多学者用"复杂性"来概括这些特点[3,4],并就此问题进行过很多有益的讨论[5,6]①。

据本文对异常及其阶段性的认识,利用岩石力学实验和数值模拟结果来讨论不同阶段异常分布的特征。

2 异常与异常阶段性

地震前是否会出现异常归根结底是一个力学问题。一个观测点出现异常是由于外界力学条件变化在该点引起的力学扰动而造成的。这些力学扰动在一些地点可能引起力学失稳而发生地震,在另一些地点则可能仅仅引起一些异常。当异常出现在某点发生地震前,则被称为

* 国家地震局"八五"攻关项目(85040602)。

① 张超等,1994,我国大陆断层现代形变与地震活动关系的研究:断层形变场源关系初步探讨之一,"八五"攻关项目(850406034)。

“前兆”，如果它们发生在某点发生地震后，则被称为“后效”。外界力学条件变化可由两种因素引起：其一是外部驱动力的变化，其二是区域内其它构造部位变形力学状态发生变化。这些构造部位可以是区域上的任意构造，也可能是未来的震源。由此，一个观测点或在一个区域是否出现前兆必须具备两个条件，即构造不均匀性[7]和具有强烈响应的观测点。

在完全均匀的条件下物体各个部位变形程度相同，就无所谓差异，也就无前兆。只有当物体内部由于介质和结构的不均匀引起变形程度不一致，才会在一些部位先出现显著的变形，出现所谓的“前兆”。一个构造部位的破裂连接过程是失稳前的准备阶段，即失稳发生在断层各部位匀阻化后[8]。因此，断层连接过程或匀阻过程所伴随的现象均为失稳前的过程，也可以作为“前兆”。这就不难理解，为什么在比较均匀的构造区，前兆出现的范围和幅度小，而且时段短。

观测点是否存在明显的响应，取决于该点与变形构造的关系。如果它与变形构造间存在强烈相互作用，该观测点会对构造变形产生强烈的响应。反之，如果它与变形构造间无强烈相互作用，即无构造上的相互牵连，即使空间位置邻近，也不会在该观测点产生强烈的响应。

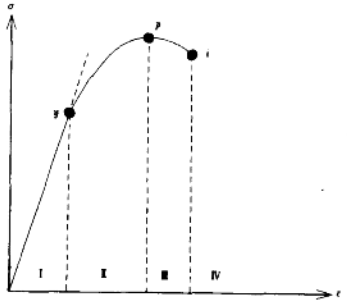

图1 岩石应力-应变曲线上的特征点与变形的阶段性

Fig. 1 The characteristic points on a stress-strain curve of rocks and the deformation stages.

不同变形阶段产生异常的力学原因不同，异常所表征的构造现象或构造内涵也不同。本文从岩石变形的标准应力-应变曲线出发来讨论地震前异常的阶段性。图1为一条常见的岩石变形曲线，曲线上有3个特征点：屈服点(y)、强度极限点(p)和失稳点(i)。由这几个点可把曲线分为4个阶段：在屈服点(y)以前为线性变形阶段(Ⅰ)；在屈服点(y)和强度极限点(p)之间为屈服阶段(Ⅱ)，这是一个非线性变形阶段，由于标本内已有局部变形，在此阶段标本内的应力场可能发生调整；在强度极限点(p)和失稳点(i)之间为临失稳阶段(Ⅲ)，在此阶段标本内的微破裂进入扩展、连接和集中化；在失稳点(i)以后进入失稳阶段(Ⅳ)。换而言之，可将强度极限点(p)以前(Ⅰ、Ⅱ阶段)称为中长期阶段。在此阶段异常是由应力增强或应力调整所引起，即使出现异常，如果外力减小，失稳可能不会发生。在强度极限点(p)以后至失稳点(i)前(Ⅲ阶段)可称为短临阶段。在此阶段异常出现与局部破裂扩展和弱化有关。由于未来的破坏区的刚度与环境刚度的比值不同，破坏又有稳态和非稳态两种。但是一旦进入这个阶段，破坏已是不可逆转，该阶段出现的异常与未来的失稳关系密切。

为了便于分析引起异常变化的原因，把应力场分为基本应力场和扰动应力场。在区域应力作用下不同构造部位附近的的应力场称为基本应力场，而由上述不同原因引起的应力变化量称为扰动场，扰动场是叠加在基本场上的增量场。如果说在无异常出现的时期，区域应力场与各构造部位是处于某种平衡状态，而扰动场的叠加就可能破坏了这种平衡，从而引起异常。例如一些构造部位可能叠加了挤压，另一些部位则可能叠加了扩容或错动。扩容区可以表现为地表拗陷、地下水位下降等；挤压区可以表现为地形隆起、地上水位上升等；剪切应力增大可能使断层位移量变化等。因此，我们可以通过分析这种叠加的增量场了解可能引起异常现象的原因。

3　构造模型与力学模型

断裂带具分段性，常见的分段形式有：摩擦系数和断层物质变化引起的分段、错位造成的雁列构造引起的分段以及方向变化造成的拐折构造引起的分段等。本文侧重研究在不同变形阶段由不同原因在雁列组合构造区引起的应力扰动场的差异。为了分析不同阶段异常出现地点不同的原因以及这些异常的分布与未来震源的关系，针对区域应力场增强，构造应力场调整以及局部构造部位弱化，断层开始扩展以至连接的全过程设计计算程序和分析。

由于本文侧重于研究构造型式对应力场的影响，故回避介质差异造成的复杂性，不同方向断层均采用同样的力学参数。考虑到自然界断层带遭受到的是大变形，因此采用几何、介质和边界三重非线性来处理变形问题[9]。断层按弹塑性处理，确定 5 个力学参数，即弹性模量 E、泊松比 ν、屈服极限 σ、材料硬化模量 E_t 及硬化参数 β。断层两侧边界取滑移面，滑移面摩擦系数相同，按接触碰撞算法处理。断层以外介质按弹性处理，只确定弹性模量 E 和泊松比 ν。断层扩展通过把有关单元由弹性介质改变为弹塑性介质来实现，断层弱化则通过降低断层介质力学参数的办法来处理。

选取最大剪应力 S_{max}（$S_{max}=(\sigma_1-\sigma_2)/2$，张力为正）和平均应力 A_m（$A_m=(\sigma_1+\sigma_2)/2$，张性为正，压性为负）来表示不同构造部位的应力。在下面所有图件中均以模型名称后面加 S 或加 A（如 EC5S，SDQ2A）表示最大剪应力和平均应力基本场，以 δ_S 和 δ_A 代表由于某种原因引起的应力扰动场（增量场），增加为正，减小为负。

4　不同原因引起的应力扰动场

4.1　基本应力场

设计了 4 组串行排列的雁列构造模型来研究这一问题。EC21 和 EC22 为一系列同类型雁

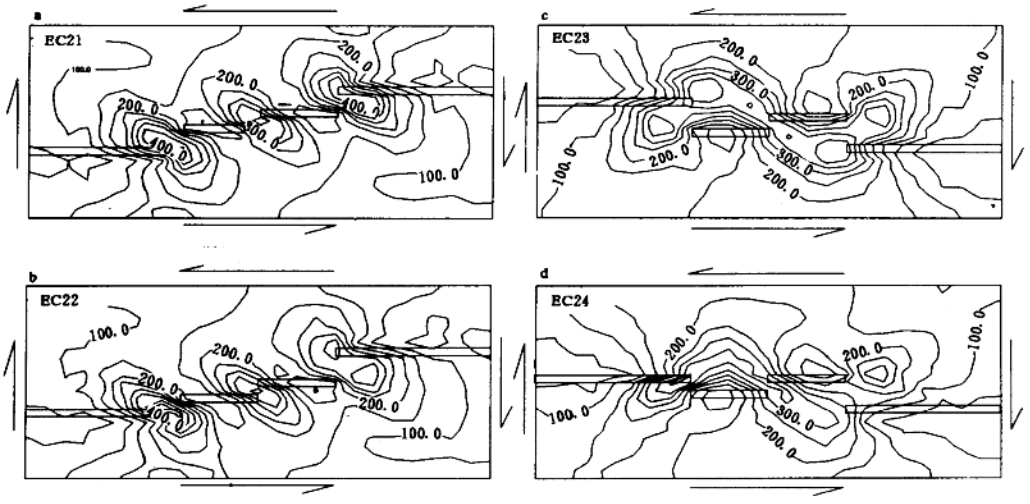

图 2　左型剪切力作用下不同雁列构造组合的最大剪应力场

Fig. 2　The maximum shear stress field on different types of composite en-echelon faults under the left-lateral shear stress.

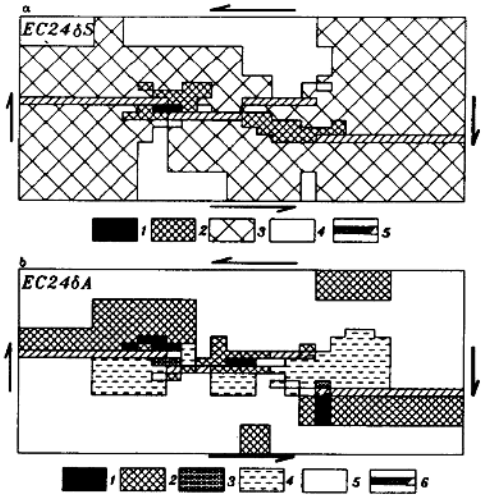

图 3 左型剪切驱动力增强引起的应力扰动场

Fig. 3 The stress-disturbant field by the raise of left-lateral shear driving force.

δ_S 最大剪应力增量：1 应力强上升区，2 应力上升区，3 应力弱上升区，4 应力微变化区，5 断层；δ_A 平均应力增量：1 强扩容区，2 扩容区，3 强挤压区，4 挤压区，5 微变化区，6 断层

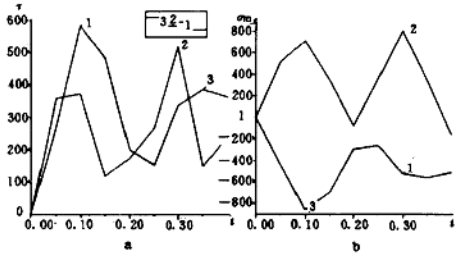

图 4 模型 EC23 在变形过程中各构造部位应力的起伏变化

Fig. 4 The stress fluctuation in different position of model EC23 during the deformation.

原因主要由外力变化引起。这里要考虑两种情形，驱动力增强及区域应力场调整。

4.2.1 用含不同雁列类型的走滑断层（模型 EC24）来说明区域应力增强引起的扰动场分布。图 3 表示当区域驱动力增加 50%时引起列构造，而 EC23 和 EC24 则为不同类型的雁列构造。所有这些模型均在平行断层方向受左型剪力，垂直断层方向受右型剪力，造成 NE 向压力，NW 向张力。图 2 表示这 4 种构造组合下最大剪应力的分布，d 值代表两雁列断层端点间垂直断层方向的距离，s 值代表端点间平行断层方向的距离，断层重叠时 s 值为正，分离时 s 值为负。由图可见，相同类型构造部位应力分布类似，而应力水平则取决于错列部位的 d 和 s 值[10]，此外，雁列构造在模型中的位置也很重要。EC21（图 2a）中 1、2、3 处同为左阶，2 处 d 值最小，最大剪应力水平最高。EC22（图 2b）中 1、2 两处 d 值相同，由于力是由边缘向中间传递的，因此，位于边缘的 1 处应力水平在早期高于 2 处。

4.2 由驱动力变化引起的应力扰动场

如前所述，在中长期阶段引起应力扰动的

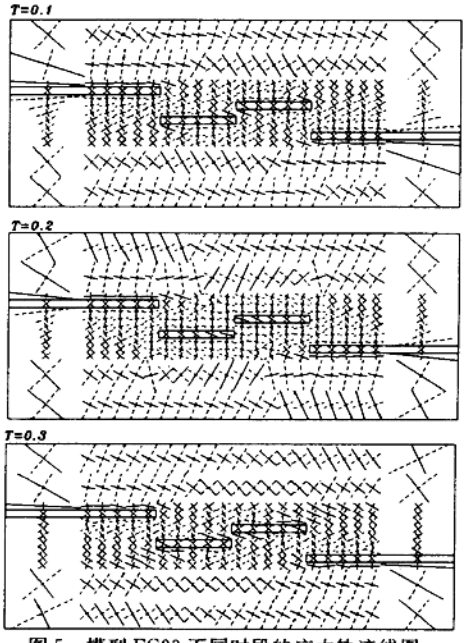

图 5 模型 EC23 不同时段的应力轨迹线图

Fig. 5 The stress trajectories of model EC23 in different time during the deformation.

实线为最大主应力方向，点线为最小主应力方向

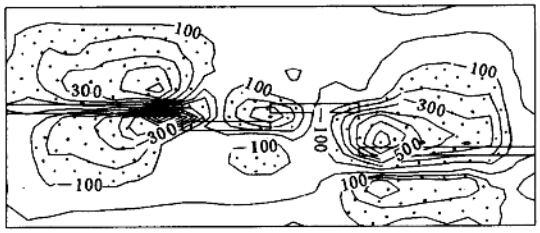

图 6　模型 EC23 中 $t=0.2$ 相对 $t=0.1$ 时的平均应力增量场

Fig. 6　The increment field of mean stress of model EC23 as comparing the value of $t=0.2$ to $t=0.1$.

细点区为挤压增强区

的最大剪应力和平均应力增量。在驱动力增大的情况下断层不同部位最大剪应力均有所增加，但是不同构造部位增加的幅度有很大差别。原来应力水平较高的几个部位如 4、2、1 号位应力增大幅度均较大，其中以 4 号位增加幅度最大(图 2)。断层带本身应力增加很少，断层带内外应力增大的幅度差别达 3 个数量级。平均应力在各点的反映不同，在左型右阶部位增加了挤压，左型左阶的部位产生了扩容。由图 3b 可见，图中有 3 处产生强烈扩容，有两处产生强烈挤压。由于应力方向没有变化，原来受张力作用的地方扩容进一步增强，原来受压力作用的地方，进一步挤压，应力变化幅度也达到 3 个数量级。由应变能密度准则[11]判断未来地震最可能发生的位置是 4 号位，但与之邻近的某些部位只有微弱变化，而与之相距较远的 2、1 号位，以及更远的部位却有较强烈的变化。由此可见，由区域应力场增强或减弱所引起的应力扰动不是均匀的。原来应力集中的地方会受到更大的扰动，但是不改变原来的应力方向。

4.2.2　用含不同雁列类型的模型(EC23)研究由驱动力调整引起的应力扰动场。当区域内存在弹塑性变形的断层带时，在驱动力和介质条件不变的情况下，随着断层的错动变形，各部位的应力水平也可以起伏变化。图 4 为模型中几个部位的最大剪应力(S)和平均应力(A)随时间的变化。取 $t=0.1$，0.2，0.3 三个时段分析，在 $t=0.1$ 时，1、3 部位应力水平高；$t=0.2$ 时，应力水平处于低谷；$t=0.3$ 时，2 处的应力水平高于 1、3 处。图 5 表示这 3 个时刻的主应力轨迹线。由图可见，随着变形的发展，各构造部位不但应力水平有变化，主应力方向也发生变化。值得指出的是在 $t=0.2$ 时模型中部应力方向变化较大。由 $t=0.2$ 相对 $t=0.1$ 时的应力增量场分析，由于 $t=0.2$ 时应力水平很低，不同部位的最大剪应力均在下降。原来应力水平高的地方应力下降量也大。由平均应力增量

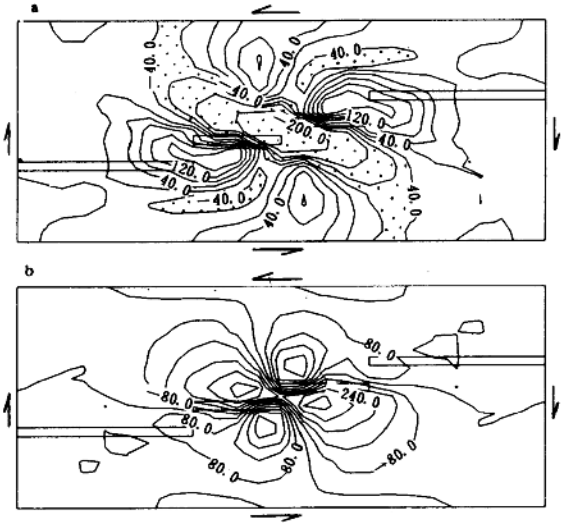

图 7　组合雁列构造中由断层扩展引起的最大剪应力(a)和平均应力(b)扰动场

Fig. 7　The stress-disturbant field by propagation of faults in a composite en-echelon model.

细点区在 a 中表示最大剪应力下降区，在 b 中以“－”号表示压缩区

图(图 6)可见,原来的扩容区变成挤压增强区(负号区,以细点表示),原来的挤压区变为扩容增强区(正值区),平均应力变化幅度很大。由此可见,区域应力场调整时随着应力水平的起伏变化可在雁列部位产生强烈的平均应力变化。同样可见,$t=0.3$ 时,1、3 部位最大剪应力下降,而 2 处应力增加。这种由于全局性的应力场调整造成的应力水平起伏影响范围均很大。

4.3 由断层扩展、弱化引起的应力扰动场

短临阶段伴随着断层扩展、连接和集中化,在此阶段应力扰动可能是由断层扩展或弱化引起。我们以上述几个模型为例研究断层扩展造成的应力扰动场,并从两方面着手,即断层扩展引起的扰动场和断层连接过程引起的扰动场。

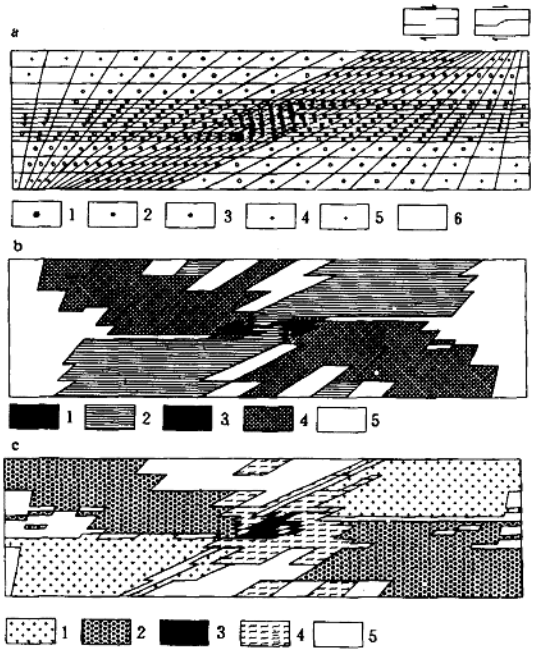

图 8 左型右阶雁列断层连接过程中最大剪应力(a)、平均应力(b)应力扰动场与平均应力变化过程分布图(c)

Fig. 8 The shear (a), mean (b) stress-disturbant field and the process of mean stress(c) during the link of faults in a L.R en-echelon model.

a 中 1 强烈下降区,2 强下降区,3 下降区,4 强上升区,5 上升区,6 微变化区; b 中 1 强压缩区,2 压缩区,3 强扩容区,4 扩容区,5 微变化区; c 中 1 持续压缩区,2 持续扩容区,3 强起伏变化区,4 起伏变化区,5 弱起伏区

4.3.1 上述几个模型中部均有长度为 10,$d=1$ 的左阶雁列,释放雁列中部单元使中间两段的断层连接。在此断层两侧为 d 值不同的同型号雁列(EC21 和 EC22)和异型号雁列 EC23 和 EC24)。

由于断层连接,应力变化首先发生在雁列连接部位,其次发生在新的连接断层的两端。以断层扩展连接部位为中心最大剪应力上升区与下降区相间分成八瓣。在与应力主轴 σ_1 和 σ_2 平行的方向为最大剪应力下降区,与它们斜交的是最大剪应力上升区。模型 EC21(图 7)和 EC22 中,连接中心部位的图案相似。但 EC24 中该部位的应力变化量明显减小。

新扩展断裂两侧的雁列处是一个应力上升部位。EC21 和 EC22 中分别有 $d=1$,$d=2$ 与 $d=3$ 的部位,$d=1$ 的部位的最大剪应力增量为 300 多,$d=2$ 的增量为 250±,$d=3$ 的为 180±,应力均比单纯的端点应力增高。几个相邻雁列构造部位,由于相互作用程度不同,应力增量不同。此外,d 值相同的异型雁列比同型雁列的增量小。

平均应力在断层扩展部位形成强烈挤压区。围绕这个部位,扩容区与挤压区呈四象限分布,不同模型在这方面是相似的。强烈扩容区垂直张力方向,强烈挤压区(负值区)垂直压力方向。但是 EC21 与 EC22 扩容量相当,而 EC24 的最大扩容量和最大挤压量小得多。除扩展区外,在连接断层两侧的同型雁列部位出现扩容区,而异型雁列部位出现的是挤压区。

4.3.2　以雁列构造连接过程为例来说明由断层连接过程引起的应力扰动场及其变化过程。地震过程往往包括局部断层扩展以及弱化扩展断层的连接、断层位移加剧至失稳。断层扩展连接是临近失稳的一个变化过程。图 8、9 分别表示右型左阶和左型左阶雁列构造,在应力作用下连接为拐折构造后产生的应力扰动场。在图 8 中断层扩展由左断层段右侧端部开始。图 8a 表示右型剪切下,左阶雁列构造失稳前最大剪应力的变化。由图可见,断层扩展段,断层段及其附近为应力强下降区或下降区,断层扩展段上下为应力上升区。由图 8b 所示,断层扩展段为强挤压区,新形成的拐折内侧为强烈扩容区,压出象限为挤压区,压入象限为扩容区。其中,扩容区中有挤压区,挤压区中也有扩容区。断层扩展段及其上下两侧为最大剪应力强烈起伏区和起伏区,在压入象限为持续挤压区,压出象限是持续扩容区,它们可反映前兆现象的变化过程(图 8c)。

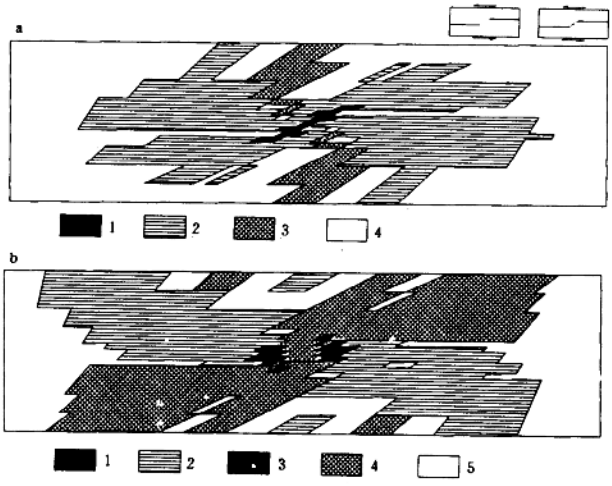

图 9　左型左阶雁列断层连接过程中最大剪应力(a)与平均应力(b)的应力扰动场

Fig. 9　The shear (a) and mean (b) stress-disturbant field by the link of faults in a LL en-echelon model.

a 中 1 强下降区,2 下降区,3 上升区,4 微变化区;

b 中 1 强压缩区,2 压缩区,3 强扩容区,4 扩容区,5 微变化区

图 9a、b 与图 8a、b 大致轮廓类似。但图 9b 与图 8b 不同的是挤压区与扩容区位置相反。

由此可见,在断层失稳前这一阶段的特点是:(1) 应力场分布复杂,但是,不论是左型还是右型,扩展断层段均为最大剪应力下降区,强烈扩容区与挤压区的分布随构造条件而变;(2) 应力变化过程复杂,应力剧烈起伏变化,起伏区主要位于扩展断层附近;(3) 应力起伏变化的幅度大,变化幅度最大的区域,其变化幅度与背景应力达同一个量级,因此这种变化应该能观测到;(4) 剧烈变化区的尺度与震源区尺度相当,起伏区可以是震源区尺度的 3～5 倍,而应力变化区的尺度更大。考虑到不同地区的具体地质条件不同,这些区域在一定地质条件下也可产生大变化;(5) 剧烈起伏的时段与断层扩展连接的时期相同,如过程发展很快,这个现象就很短暂。

5　小　结

(1) 引起区域应力扰动的原因不同,应力扰动场分布就不同。从区域应力场增强到局部断层弱化、扩展以至连接过程中不同阶段受应力扰动的构造部位不尽相同,这可能是中长期阶段和短期阶段异常出现于不同部位的原因。

(2) 由驱动力变化引起的扰动场分布范围广,异常地点可以很多,增量场与原来应力方向一致,强烈扰动区与原来的应力集中区一致,与未来震源区无必然联系。

(3) 由区域应力场调整造成的扰动场可使原来应力方向改变,应力调整对平均应力影响

极大，强烈扰动区位于断层错列部位。

(4) 在雁列组合中，局部断裂扩展造成的扰动场以扩展部位为中心，与之相伴的是平均应力扰动场的四象限分布和最大剪应力扰动场的八瓣式分布。扰动量随断裂扩展部位间的距离增加而衰减。应力扰动区随扩展后的断层长短而变化。局部断裂的扩展对串行排列的相邻雁列部位也产生应力扰动，扰动量明显高于无断层的部位。而相邻雁列部位的应力扰动场随扩展部位的雁列类型相同否而变化，在相邻部位存在异型雁列时，应力扰动量变小。

(5) 在断层失稳前的扩展连接过程中，断层扩展区最大剪应力会下降；强烈扩容区与挤压区的最大剪应力分布随构造条件而变化。这个阶段的最大特点是由于断层的持续扩展，震源区附近应变出现剧烈起伏。剧烈起伏区的范围与震源尺度相当或稍大，而起伏区可以是震源尺度的 3～5 倍。广大区域则可以出现持续扩容区和挤压区。

看来，当区域出现异常并确认不是干扰时，首先要分析引起异常的原因，如果是由区域应力场变动引起的异常则只需密切注意发展动态，因为区域应力增强不一定意味着地震，不能由于其分布区大，出现异常类型多就判断将有大震。如果在其中一个变化区的应力增量场发展成八瓣式和四象限式分布，则可以认为该处断层开始弱化或扩展，进入了孕震阶段，断层破坏进入不可逆转阶段。这时尚需密切注意断层扩展速率、应力场起伏变化幅度以及沿断层带扩容挤压相间分布等情况，才能判断是否将以地震方式释放能量。

区域构造十分复杂，这里仅以常见的雁列构造组合型式为例，说明不同阶段地震前异常场的分布形态，尚需结合具体区域的构造和台站分布把这项研究引向深入。

(1995 年 6 月收稿，1995 年 8 月改回)

参 考 文 献

1 马宗晋，傅征祥，张郧珍，等. 1966～1976 年中国九大地震. 北京：地震出版社，1982.

2 冈田义光. 地震预报：经验性抑或确定性关于内陆直下型地震预报的方向. 许绶平译. 国际地震动态，1994，(2)：18～21.

3 国家地震局<一九七六年唐山地震>编辑组. 一九七六年唐山地震. 北京：地震出版社，1982.

4 梅世蓉，冯德益，张国民，等. 中国地震预报概论. 北京：地震出版社，1993.

5 秦保燕，郭增建. 场源前兆的判别：λ 型在地震预报中的应用前景. 内陆地震，1993，7(4)：309～318.

6 Моргунов В А. К проблеме оперативного прогноза землетрясений Док. АН СССР 1991，319(1)：138～142.

7 大中康誉. 在物理定律基础上建立预报理论的方案. 彭岩译. 国际地震动态，1994(1)：26～28.

8 王绳祖. 强震危险区的多判据原理. 现代地壳运动研究(4). 北京：地震出版社，1984. 10～17.

9 陈开平. 一种非线性动态断层力学模型. 地震地质译丛，1993，15(3)：18～22.

10 Ma J，Du Y，Liu L. The instability of en-echelon cracks and its precursors. J Phys Earth，1986，34(Suppl)：S141～S157.

11 Du Y，Aydin A. The maximum distortional strain density criterion for shear fracture propagation with applications to the growth paths of en echelon faults. Geophys Res Lett，1993，20(11)：1091～1094.

THE STAGES OF ANOMALIES BEFORE AN EARTHQUAKE AND THE CHARACTERISTICS OF THEIR SPATIAL DISTRIBUTION

Ma Jin　　Ma Shengli　　Liu Liqiang
(*Institute of Geology, SSB, Beijing* 100029)

Abstract

The complication of tectonics in China gives us an advantage to find some anomalies near or far from the coming earthquake. They may be alert to the occurrence of a strong earthquake. However the problems are: 1) before some strong earthquakes there were no anomalies, 2) in some cases no earthquake occurred after the anomalies, and 3) in some cases the place with obvious anomalies did not correspond to the epicenter. Therefore, studying the stages of anomalies and analysing the cause and spatial distribution may help us to elucidate the problems.

The deformation process in a region may be divided into 4 stages: stage Ⅰ is before the yield point, and stage Ⅱ is between the yield point and peak strength point. Stages Ⅰ and Ⅱ may be related to the long-term to medium-term stages before earthquake. Stage Ⅲ is between strength point and instable point and stage Ⅳ is after instable point. Stage Ⅲ may be related to the short-term to imminent stages before earthquake. The anomalies appearing in stages Ⅰ and Ⅱ may be caused by the change of driving force and the anomalies in stage Ⅲ may be caused by the propagation or weakening of the fault and smoothening of the fault surface.

A numerical modelling has been made to study the spatial distribution of anomalies in each stages. In order to reveal the distribution and its causes more clearly, the increment mean stress $\delta\sigma_m$ and the increment maximum shear stress $\delta\tau_{max}$ are calculated. It is shown that the distribution of $\delta\tau_{max}$ in stages Ⅰ and Ⅱ is similar to the background stress field. The distribution of $\delta\sigma_m$ in stage Ⅱ is outstanding on the en-echelon jogs. the distribution of $\delta\tau_{max}$ and $\delta\sigma_m$ display an eight-petaline pattern and a four-quadrant pattern, respectively, the propagation point is in the center of the pattern. The temporal process of the distribution of the increment stress field in an en-echelon fault system has also been studied.

Key words: Earthquake precursor, Anomaly recognition, Long-term anomaly, Medium-term anomaly, Short-impending anomaly, Spatial distribution characteristic

第 17 卷 第 4 期
1995 年 12 月

地 震 地 质
SEISMOLOGY AND GEOLOGY

Vol. 17 No. 4
Dec. 1995

复杂构造应力扰动场与发震构造识别问题的研究*

马 瑾 刘力强 马胜利 邓志辉
(国家地震局地质研究所, 北京 100029)

摘 要 在地震短临阶段异常是由局部断层扩展或弱化引起。实验与数值模拟结果曾得到与之相伴的是平均应力扰动场的四象限分布和最大剪应力扰动场的八瓣式分布。为检验此结果的普适性作了进一步的研究。结果表明不论区域构造及其基本应力场如何复杂,这种四象限分布与八瓣式分布型式不变,这为最终判定失稳区提供了依据。与此同时,在复杂构造情况下这种应力扰动场的畸变也不容忽视。

主题词: 发震断层 异常识别 空间分布特征 应力场 数字模拟

1 问题的提出

唐山地震前地下水位[1~3]、水氡含量和形变电阻等[4~5]在临震前出现四象限分布,震中位于四象限节线的交点附近。通海地震前应变场也有类似的特点[6]。这些文献强调了异常现象的有序象限分布,及其出现时间临近发震。如以唐山地震来说,这种分布出现在震前几小时至 1~2d。在实验室也曾得到过破裂前后应变场四象限分布图象[7]。近期,笔者[8]又以组合雁列构造为例,研究由不同力学原因引起的应力扰动场的分布特征,也发现由于断层扩展引起的应力扰动场具有平均应力四象限和最大剪应力八瓣分布特征。地壳构造十分复杂,在复杂构造组合下,上述分布特征是否还能作为断层扩展或弱化的标志,尚值得研究。

为了便于分析引起异常变化的原因,把应力场分为基本应力场和扰动应力场。我们把区域力作用下不同构造部位附近的应力场称为基本应力场,而把由上述不同原因引起的应力变化量称为扰动场,扰动场是叠加在基本场上的增量场,故也可称为增量场。考虑到复杂构造的基本应力场是十分复杂的,其中包含了由构造和介质引起的很多不均一性,而它们的增量场中扣除了这些不均一性引起的复杂性,突出了由断层扩展、弱化前后的差异变化,使现象更加明显。本文拟利用数值模拟方法研究破裂扩展后应力场相对扩展前的增量场的分布特征。

考虑到自然界断层带主要遭受到的是大变形,计算中采用几何、介质和边界三重非线性来处理变形问题的有限元模型[9]。断层按接触碰撞算法处理,计算方法及参数的选取与文献

* 国家地震局"八五"攻关项目(85040602)。

Spatial Distribution of Anomalies in Different Stages before an Earthquake

JIN MA, SHENGLI MA and LIQIANG LIU
Institute of Geology, State Seismological Bureau, Beijing, 100029, China

Abstract

A deformation cycle in a region may be divided into 4 stages, corresponding to long-term, medium-term, short-term to imminent stages before earthquake and instability, respectively. Anomalies appearing in stages I and II may be caused by changes in driving force and anomalies in stage III may be caused by fault propagating or fault weakening. In order to reveal distribution of anomalies in different stages, increments of mean stress and maximum shear stress for models with en-echelon faults and other fault patterns are studied numerically. It is shown that distribution of increment of maximum shear stress in stages I and II are similar to the background stress field while variation of incremental mean stress in stage II is outstanding at en-echelon jogs. Distribution of incremental maximum shear stress and incremental mean stress display an eight-petaline pattern and a four-quadrant pattern, respectively, surrounding the propagation area in stage III. The eight-petaline pattern, four-quadrant pattern and strong undulating of dynamic characteristics in mean stress may help to distinguish possible upcoming unstable fault.

Keywords: earthquake precursor, anomaly recognition, short-impending anomaly, numerical modelling

INTRODUCTION

A lot of observatory stations have been setting up in China since Xingtai earthquake (1966) in order to grasp earthquake precursors. Anomalies that persist for periods of a few even ten years prior to an earthquake in a region are called "long to medium-term precursors". Those appearing in periods of a few months to a few days before an earthquake are called "short-term or imminent precursors". On the other hand, anomalies appearing in vicinity of the epicenter are referred to as "source precursors ", and those appearing in a rather large area as "area precursors". The complication of tectonics in China gives us an advantage to observe some anomalies near or far from the epicenter of an upcoming earthquake, which may be an alert to the occurrence of a strong earthquake. However, earthquake cases indicate that (1) there were no anomalies before some strong earthquakes, (2) in some cases no earthquake followed the anomalies, (3) places with "long to medium-term precursors" often did not correspond to places with "short-term to imminent precursors", and (4) places with obvious anomalies did not always correspond with epicenter of upcoming strong earthquake. These phenomena show that both "universality" and "regionality" in earthquake precursors may exist at the same time, which have been discussed by many authors[3-4,9-15]. We suggest that anomalies in different time scales may be caused by different mechanisms, which are related with deformation stages. Therefore, studying spatial distribution of anomalies in different stages and corresponding mechanisms may help us to understand above mentioned phenomena. In this paper, we will try to give some discussions on this topic based on mechanical behavior of rocks and some numerical results.

ANOMALIES IN DIFFERENT DEFORMATION STAGES

It is intrinsically a problem of mechanics whether anomalies appear or not. Anomalies appearing at an observatory are attributed to the mechanical interference from changes in external mechanical condition. The interference may cause an earthquake as a result of mechanical instability in some place but only anomalies in other places. Changes in external mechanical condition may be caused by different mechanisms, such as change in external driving force, deformation of some tectonic elements easy to be deformed and propagating or weakening of faults in a region. Such an element may become seismogenic fault in future or not. Evidence indicates that regions with heterogeneity in tectonics and spots having strong interaction with deformed elements are favored by anomalies.

In case of homogeneous fault, there is no great difference in deformation along fault, hence no obvious precursor. However, for heterogeneous fault system strong deformation may appear in some segments earlier, which may act as precursors of a strong earthquake. The linking of fault segments is a preparing stage for instability, and instability occurs after uniformization of sliding resistance. Therefore, anomalies appearing in both linking of faults and uniformization of sliding resistance may be regarded as "precursors".

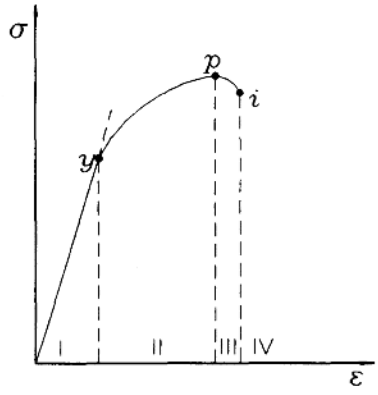

Figure 1. The characteristic points on a stress-strain curve of rock and the deformation stages

Deformation stages and corresponding anomalies can be discussed based on a common stress-strain curve of rock (Fig.1). There are three characteristic points in the curve: yield point (y), strength point (p) and unstable point (I), which may divide the curve into four stages by them. The first one before yield point (y) is linear deformation stage (I). The second one between point y and strength point (p) is nonlinear deformation stage (II), in which the stress field may be redistributed due to locally inhomogeneous deformation. The third one between point p and unstable point (i) is critical stage (III), in which propagating, concentrating and linking of microcracks are predominated. The fourth one after point i is unstable stage (IV). In other words, the stages before point p (stages I and II) may be taken as long to medium-term ones. Anomalies appearing in these stages may be caused by changes in driving force or redistribution of stress field. Even though anomalies appear in these stages, instability may not occur if driven force decreases again. The stage III may be regarded as short-term to imminent ones. Anomalies appearing in this stage are related with propagating, weakening and linking of cracks. The failure may be stable or unstable depending on the ratio of stiffness in failure area to that in surrounding area. However, the failure is unreversible once the deformation enters this stage. Anomalies in this stage are closely related to upcoming stable or unstable failure.

In order to understand distribution of anomalies, stress field is divided into essential and incremental ones. The former means background stress field in a region by the action of regional driven force and the latter means variations in stress in some period caused by mechanisms mentioned above. Consequently, incremental stress field is a disturbed field superimposed on essential one. In case of absence of anomalies, the regional stress field may be regarded as being in steady state. Superimposition of disturbed stress field will break the state and cause anomalies. Therefore, incremental field can indicate clearly distribution and mechanism of anomalies.

A natural fault system is usually inhomogeneous both in geometry and in material, which may affect evolution of stress field, hence anomalies. In this paper, we focus on effect of geometric texture neglecting that of material. We chose en-echelon faults, the most common fault geometry, as geometric models and study distribution of disturbed field in different stages caused by different mechanisms including change in driving force, redistribution of regional stress field, fault propagating and so on.

Considering that a natural fault zone may be nonlinear in geometry, material and boundary[1,5-7], the triple-nonlinear method is used to deal with deformation along fault. The mechanical behavior of faults is considered as a contact problem and is simulated by a contact-impact algorithm, which permits gaps and sliding along material interface. Fault gouge is considered as a elasto-plastic material with five mechanical parameters including elastic module *E*, Poisson ratio ν, yield limit σ, hardening module *Et* and hardening ratio β. Surrounding rock is considered as an elastic material with two parameters including elastic module E and Poisson ratio *v*. In calculation, fault propagating is achieved by changing some elements from elastic to elasto-plastic behavior, and fault weakening by decreasing the modules of fault gouge.

In this paper, define extensional stress as positive and compressional stress as negative, and maximum shear stress $\tau_{max} = (\sigma_1 - \sigma_2)/2$, and mean stress $\sigma_m = (\sigma_1 + \sigma_2)/2$. Essential fields of maximum shear stress and mean stress are expressed by the model name with τ and σ_m (e.g. EC5τ, SDQ2σ_m), respectively. Correspondingly, disturbed stress fields are expressed by δτ and $\delta\sigma_m$.

DISTURBED STRESS FIELD CAUSED BY DIFFERENT MECHANISMS

Essential Stress Field

Four models with complex en-echelon faults are designed to study this problem. EC21 and

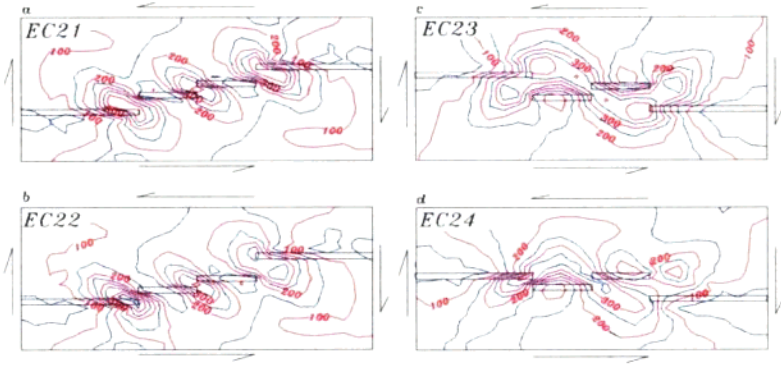

Figure 2. The maximum shear stress field for models with different complex en-echelon faults.

EC22 are models with the same type of en-echelon faults and EC23 and EC24 with different type of en-echelon faults. All models are applied by the left- lateral shear in direction parallel to the fault strike and right-lateral shear in direction perpendicular to the strike. The maximum shear stress fields for these models are shown in Fig.2. For convenience, distances between two inner ends of en-echelon faults in direction perpendicular and parallel to faults are indicated by *d* and *s* respectively[8]. Take *s* as positive for overlapping en-echelon jog and negative for separating jog. It is clear from the figure that stress distribution in similar textural elements is similar, and stress

level is dependent on d and s of jog and its position in model. For example, all jogs (1, 2 and 3, see Fig.4) are left steps in model EC21, where jog 2 with smallest d-value is of highest level of maximum shear stress. In model EC22 (Fig.2b), d-values in jog 3 and 2 are the same, but stress level in jog 3, close to border of the model, is higher than that in jog 2 in early stage because force is transmitted from border to center.

Disturbed Stress Field Related to Change in Driving Force

Distribution of $\delta\tau_{max}$ and $\delta\sigma_m$ for model EC24 caused by increase of driving force (by 50%) is shown in Fig.3. It can be seen that the maximum shear stresses in all positions increase with different levels. The higher the essential stress is, the higher the increment is. For example, jog 3 with largest essential stress is of largest incremental stress. Incremental stress within fault zone is 3 orders lower than that in outsides of fault zone. Increment of mean stress is different in different positions. In this model, increment of mean stress shows compressional in right step jog but dilative in left step jog. Three intensively dilative areas and two intensively compressional areas exist. As the orientation of stress trajectories keeps constant, the area extended originally develops further dilation and that compressed originally develops further extrusion. Possible upcoming instability may occur in jog 3 according to maximum distortional strain density criterion[2]. Variation of stress in some positions near jog 3 is very weak, but variation in jog 1 and 2 and other positions may be strong. This indicates that stress disturbance caused by change in driving force is not distributed homogeneously. More strong stress disturbance occurs at positions with original stress concentration.

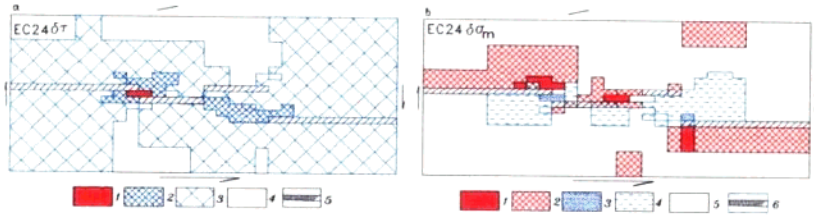

Figure 3. The disturbed stress field caused by raise of driving force. $\delta\tau$ is increment of maximum shear stress: 1 strongly elevated, 2 elevated, 3 weak elevated, 4 weak variable, 5 faults; $\delta\sigma_m$ is increment of mean stress: 1 strongly dilative, 2 dilative, 3 strongly compressive, 4 compressive, 5 weak variable, 6 faults.

Disturbed Stress Field caused by Redistribution of Stress

Disturbed stress field caused by redistribution of stress for model EC23 and EC24 is studied. In case of existence of elasto-plastic faults, stress level in different positions varies during deformation and sliding along the faults, though the driving force keeps constant. Variations of maximum shear stress and mean stress in some jogs with time are shown in Fig.4. When t=0.1, shear stress level in jog 1 and 3 is high, and when t=0.3, shear stress level in jog 2 is higher than that in jog 1 and 3. It is clear that at t=0.2, there is a decrease in maximum shear stress at all positions compared with that at t=0.1. Variation in mean stress is rather strong, and originally dilative area changes to compressive one (denoted by dots) and originally compressive area changes to dilative one (Fig.4 and 5). Strong variation in mean stress occurs in en-echelon jogs.

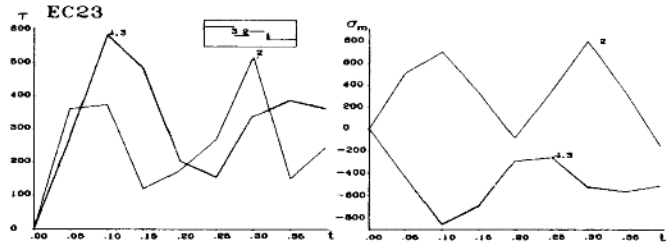

Figure 4. The stress fluctuation in different positions of model EC23 during the deformation

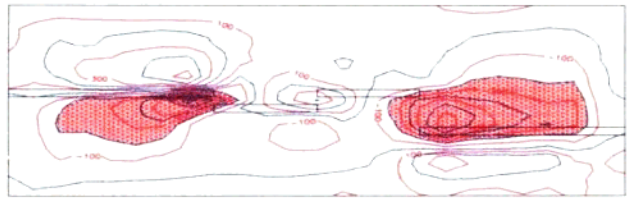

Figure 5. The increment field of mean stress of model EC24 as comparing the value of t=0.2 to t=0.1. Dotted areas indicate compression increasing area.

Trajectories of stress axes at these three moments are shown in Fig.6. It can be seen that not only stress level but also orientation of stress axes vary with time. For example, orientation of stress axes at t=0.2 are quite different from that at other times.

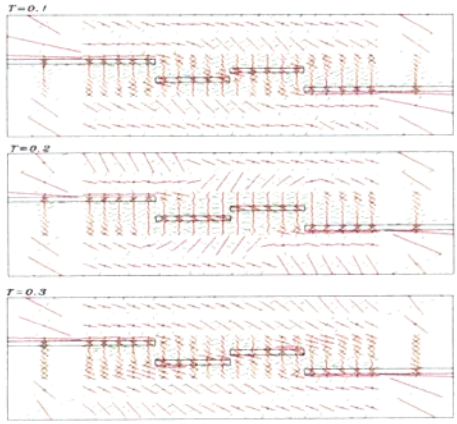

Figure 6. The stress trajectories of model EC23 in different time during the deformation. Solid and dashdot lines indicate orientations of maximum and minimum principal stress, respectively.

Disturbed Stress Field Caused by Fault Propagating and Weakening

In all models, there is a left step en-echelon jog with fault length of 10 and d=1 in center (i.e. jog2). We change elements in this jog from elastic to elasto-plastic and make faults linked to study the disturbed stress field. In this case stress variation transmits from linked area (jog2) to two ends of linked faults (jogs 3 and 1). Areas with rising and descending in maximum shear stress are distributed alternately as an eight-petaline pattern surroun-ding the linked elements. Areas with descending in τ_{max} are distributed in directions parallel to principal

stresses "σ_1" and "σ_2" and areas with rising in τ_{max} are in oblique directions to them (Fig.7a). Dilative and compressive areas are distributed as a four-quadrant pattern surrounding the linked elements in disturbed stress field of mean stress (Fig.7b). Two dilation quadrants align in direction perpendicular to extensional axis and two compressive quadrants in direction perpendicular to compressional axis. Strong descending in τ_{max} and σ_m (that means more compressive) occurs in the propagating and linked elements.

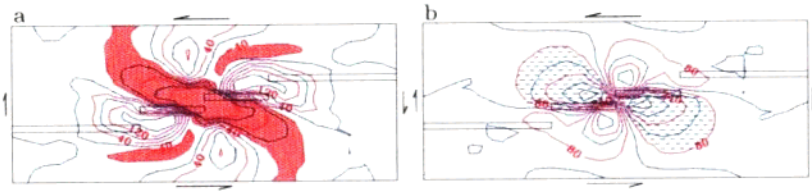

Figure 7. The disturbed stress field caused by propagation of faults in model EC22. Dotted areas in (a) are areas with descending in maximum shear stress, dashed areas in (b) are areas more compressed.

It is Interesting to indicate that such eight-petaline pattern and four-quadrant pattern of incremental field for maximum shear stress and mean stress have been distinguished not only for en-echelon fault system but also for parallel fault system, bend fault and intersecting fault system. It seems that no matter how complicated the fault system and the stress fields are, the disturbed stress fields always show such patterns as long as the propagation or weakening occurs along a fault. This result provides us a basis to distinguish possible coming unstable fault.

Dynamic Characteristics during Fault Propagating

Preparing process of an earthquake includes propagating and weakening of faults, linking of faults, accelerative slip along fault and so on. All these processes are just prior to instability. Fig.8 shows a disturbed stress field with different dynamic characteristics in a model with left

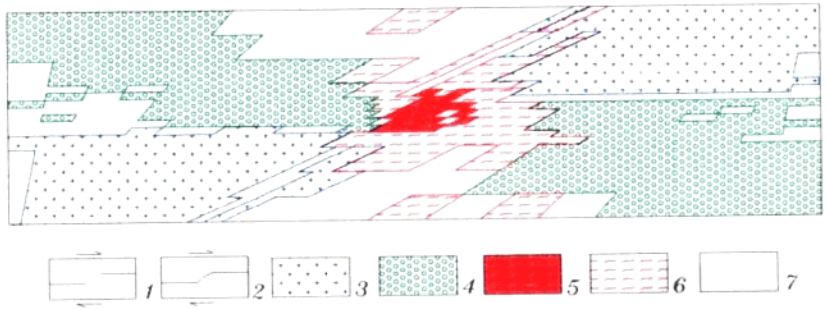

Figure 8. Dynamic process in mean stress during linking of faults in en-echelon faults. 1 and 2 denote initial and terminal states of faults, 3 continued compressive, 4 continued dilative, 5 strongly undulating, 6 undulating, 7 weak undulating.

step en-echelon faults caused by fault linking under a right lateral shear. The fault propagating begins at the right end of the left fault. The disturbed stress field of maximum shear stress and mean stress keep the same patterns as eight-petaline and four-quadrant patterns, respectively.

dynamic characteristics in mean stress with time, that is, continued compressive, continued dilative, strongly undulating, undulating and weak undulating process. Continued compressive and dilative types occur roughly in compressive and dilative quadrants, respectively. Undulating type is distributed along the propagating fault and its vicinity. Before Tangshan earthquake in 1976 there was a case history about strongly undulating of water table in a well near the seismogenic fault.

The characteristics in this stage may be summarized as follows: (1) Though essential stress field may be complicated, but disturbed stress fields always keep constant patterns, that is, eight-petaline pattern for $\delta\tau_{\max}$ and four-quadrant pattern for $\delta\sigma_m$. Area with strong descending in maximum shear stress and strongly compressive area are located on propagating segment of faults. (2) During fault propagating, changes in stress are very complicated. There are 5 types of dynamic characteristics. Among them, the strongly undulating areas are distributed along the propagating segment and its vicinity. (3) The magnitude of undulation in strongly undulating area can reach that of the essential field. Scale of the strongly undulating area is similar to that of propagating segment, while scale of undulating area is its 3 to 5 times. Stress undulating period coincides with fault propagating period. Its persisting time depends on the propagating rate.

CONCLUSION

Disturbed stress field may be caused by different mechanisms, such as increasing in driving force, stress redistribution, and fault weakening, propagating and linking. Spatial distribution of incremental stress field caused by them is different. This may be the reason for the departure of anomalies in different stages.
The disturbed stress field caused by change in driving force is widely distributed. Orientations of stress axes keep constant and strongly disturbed areas coincide with original areas with stress concentration. However, there is no inevitable relation between strong disturbed area with upcoming hypocenter.

Stress redistribution may change orientation of principal stress axes somewhere and strongly affect mean stress field, specially in en-echelon jog.

Disturbed stress field caused by fault propagating and linking has an eight-petaline pattern for increment of maximum shear stress and a four-quadrant pattern for increment of mean stress.

There are five types of dynamic characteristics in stress disturbance accompanied with fault propagating and linking. Strongly undulating area coincides with propagating segment and their space scales are almost the same.

REFERENCES

1. D.J.Benson and J.Q.Hallquist. A simple rigid body algorithm for structural dynamics programs, International Journal for Numerical Methods in Engineering, **22**, 723-749(1986).
2. Y.Du and A.Aydin, The maximum distortional strain density criterion for shear fracture propagation with applications to the growth paths of en-echelon faults, Geophys. Res. Lett., **20(11)**, 1091-11094 (1993).
3. Edition group for "Tangshan earthquake in 1976", Tangshan earthquake in 1976, (in chinese), Seismological Press, Beijing, (1982).
4. X.Gao. The precursor process and its field-source features of Datong-Yanggao earthquake, in "The selected papers of earthquake prediction in China", Seismological Press, 195-205 (1996).
5. J.Q.Hallquist. A procedure for the solution of finite deformation contact-impact problems by the finite element method, University of California, Lawrence Livermore National Laboratory, Rept. UCRL-52066(1976).
6. J.Q.Hallquist. Theoretical manual for DYNA3D, University of California, Lawrence Livermore National